

Comparative study between electromagnet and permanent magnet rails for HTS maglev

Yuyan Wen , Ying Xin , Wei Hong , Chaoqun Zhao and Wenxin Li

School of Electrical & Information Engineering, Tianjin University, Tianjin, People's Republic of China

E-mail: wenny0309@qq.com

Received 10 October 2019, revised 16 January 2020

Accepted for publication 24 January 2020

Published 12 February 2020



CrossMark

Abstract

In this study, we investigated the magnetic levitation characteristics of a high-temperature superconducting (HTS) bulk with both permanent magnet guideway (PMG) and electromagnet guideway (EMG). Trying to have the magnetic fields of the two kinds of guideways with a similar structure, then the central magnetic flux density B_z and unit magnetomotive F_u were selected as the evaluation indexes respectively for the comparative study. Different magnetic field characteristics on magnetic levitation performance were studied, such as the gradient of magnetic flux density and magnetic flux density component in different directions. Several experiments were carried out at different magnetic field conditions by changing the exciting current of EMG or replacing different PMG specimens. The experiments were conducted with a high-precision force-measuring platform. The experimental results show that the EMG has several different characteristics as compared with PMG. As a result, the magnetic levitation performance is related to the gradient of magnetic flux density as well as the directional magnetic flux density components. The structure of the magnetic field also has great influence on the performance. The results will be helpful for further study of the properties of HTS maglev and provide guidance for the subsequent EMG design.

Keywords: HTS maglev, permanent magnet guideway, electromagnet guideway, levitation force, guidance force

(Some figures may appear in colour only in the online journal)

1. Introduction

Since the discovery of high temperature superconducting (HTS) phenomenon, HTS materials have attracted extensive interest in superconducting maglev studies [1–9] due to their unique properties. The interaction between an HTS bulk and a magnet guideway can produce both vertical levitation force and lateral guidance force, which is the unique feature of HTS maglev [10]. The Meissner effect and pinning effect of an HTS bulk can provide the levitating and guiding functions without the need of a complex control system in theory [11]. In general, the characteristic of levitation force and guidance force are affected by numerous factors, such as the levitation gap [12], the lateral displacement [13], the field cooling height [14], etc It means that the levitation force performance can be regulated by changing the magnetic field characteristics, such as peak value, magnetic field component in different directions, and the magnetic field gradient, etc

Therefore, it is of great significance to analyze the relationship between magnetic field characteristics and levitation force performance.

Traditionally, permanent magnet guideway (PMG) has been used to provide an external magnetic field for HTS bulks in the magnetic levitation experiments [15]. PMG has many advantages, such as small size [16], easy to assemble [17], reasonably high magnetic field [18], etc However, a number of disadvantages accompany with PMG. For instance, the change of magnetic field strength can only be realized by applying permanent magnets with different surface magnetic flux density or different arrangement [19]. It means that once the guideway is built, the field strength and distribution cannot vary. Also as time goes on, the magnetic field will attenuate [20]. Furthermore, measures need to be taken all the time to avoid magnetic materials dropping on the guideway [21]. In the long term, the scope of application of PMG is very limited. Compared with the PMG, electromagnet

guideway (EMG) have more diverse methods to improve the performance of levitation force. As for the EMG, different magnetic field strength can be achieved by changing the value or the variation rate of the exciting current. When designing the EMG, the reasonable guideway model design can make the HTS bulk have higher magnetic field intensity and more suitable magnetic field distribution. As the guideway model built, the levitation force performance of the HTS bulk can be improved by increasing the magnitude and the change rate of the current. The polarity of electromagnet can also be changed by reversing the direction of the exciting current. Consequently, high flexibility and practicability can be attained with the same EMG. In principle, EMG can adopt a segmented instant excitation mode to realize a minimum levitation power loss as well as sufficient levitation and guidance forces for the train. The segmented instant excitation mode allows to energize the section of EMG where the vehicle reaches and power off as the vehicle has passed. Moreover, the excitation current of EMG can be adjusted to meet the needs of HTS vehicles with different loads.

To investigate the advantages and feasibility of the replacement of PMG with EMG in HTS maglev, we have carried out this comparative study. In fact, it is impossible to construct PMG and EMG with exactly the same magnetic field distribution. Even if building exactly the same EM and PM model and arrange the model in exactly the same way. Moreover, if identical magnetic fields are constructed, their levitation properties must be the same. Furthermore, only the magnetic field structure in the HTS bulk working area (shown in the red frame in figure 1) are concerned. Therefore, based on the difference, it is meaningful to construct the same magnetic field trend, select reasonable evaluation indicators, and then optimize the design of PMG and EMG under the specific indicator according to different actual needs. In this study, several groups of experiments were conducted. To make meaningful comparisons, the same central magnetic flux density B_z or the same unit magnetomotive F_u on both PMG and EMG specimens were accomplished during force measurement. By doing this, we can assume that both the PMG and EMG have similar magnetic field structures. Based on the experimental results, the key magnetic field factors affecting the levitation force performance were discussed in this paper. Furthermore, the magnetic levitation characteristics of PMG and EMG are analyzed and compared.

2. Experiment

In order to compare the magnetic levitation performance between EMG and PMG, two sets of experiments were designed. In these experiments, several tests of PMG or EMG were carried out. In the plan of these comparative tests, it is necessary to make the HTS bulk locate in the area with the same magnetic field direction and the similar magnetic field structure, which can be realized by electromagnet structure design and permanent magnet arrangement appropriately.

Based on the fundamental \square -shaped electromagnet, when the EMG is dedicated to rail transit, its design

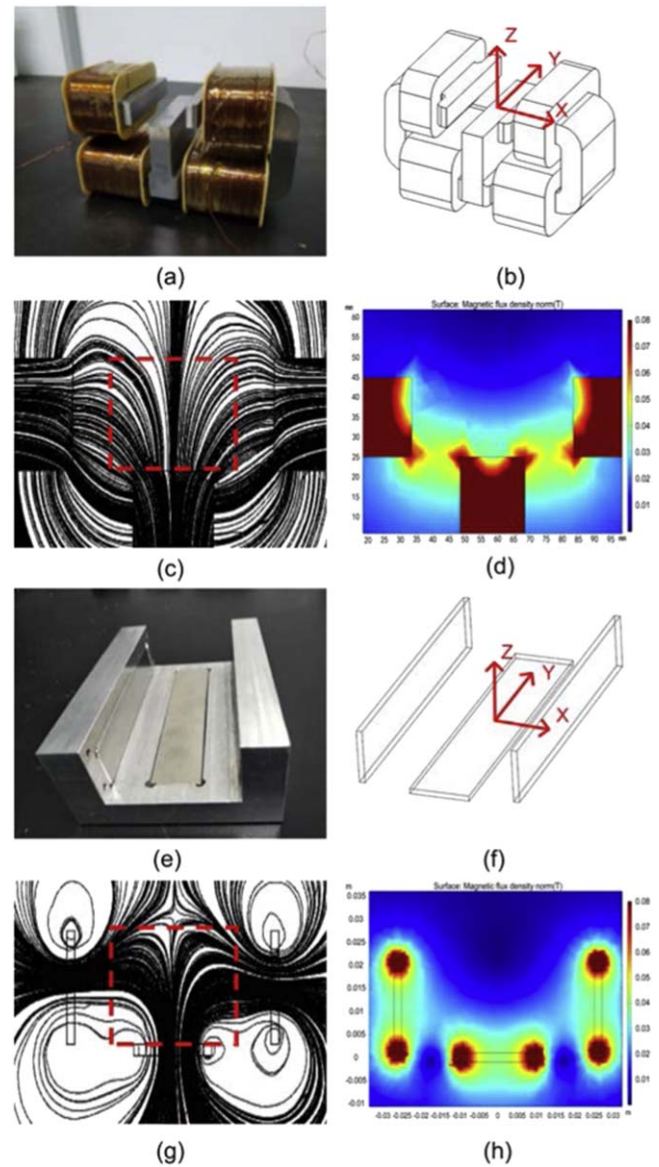


Figure 1. Photo-picture, 3D direction diagram, magnetic flux pattern, magnetic field distribution profile (simulated with COMSOL) of the EMG with current of 0.53 A and PMG (take specimen 1 as example). (a) The photo of EMG. (b) The three-dimensional coordination of EMG. (c) The two-dimensional cross-sectional view of magnetic flux distribution of EMG. (d) The magnetic field distribution profile of EMG. (e) The photo of PMG specimen 1. (f) The three-dimensional coordination of PMG specimen 1. (g) The two-dimensional cross-sectional view of magnetic flux distribution of PMG specimen 1. (h) The magnetic field distribution profile of PMG specimen 1.

consideration must follow the principles of both basic electromagnet and rail construction.

Principle 1: For the electromagnet, the iron core should not reach its deep saturation state at work time.

Principle 2: For the rail construction, the magnetic field along the driving direction must be as homogeneous as possible. The electromagnets should be able to form a guideway without apparent flaw of magnetic field at the joint of electromagnets.

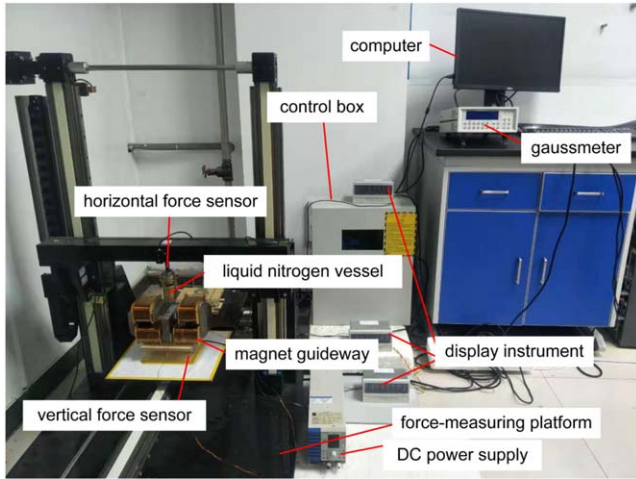


Figure 2. The photo of our HTS maglev measurement system.

Principle 3: The magnetic distribution should accord with the requirements of fine levitation performances of HTS bulk.

Correspondingly, a PMG model with the same relative position and section size is constructed, and then secured by an aluminum frame.

The relevant simulation results are shown in figure 1. Figures 1(a) and (e) are photo pictures of EMG and PMG (take PMG specimen 1 as an example). Figures 1(b) and (f) are the schematic drawings of three-dimensional coordination of EMG and PMG. Figures 1(c) and (g) are the schematic drawings of two-dimensional cross-sectional view of magnetic flux distribution of EMG and PMG. Figures 1(d) and (h) are the magnetic field distribution profiles of the EMG and PMG. The magnetic field distribution profiles are the results of computer simulation with COMSOL Multiphysics. It is easy to see that the magnetic field structure is similar in the red region. This region can be considered as a cuboid with a length of 100 mm, a width of 30 mm and a height of 20 mm. Based on the above simulation results, central magnetic flux density B_z and unit magnetomotive F_u were selected as evaluation indexes respectively. The definition of unit magnetomotive F_u is given below (formula 1 and 2). Then we carried out experiment 1 and experiment 2 at working heights (WHs) of 3, 5, and 7 mm to analyze the HTS maglev performance of PMG and EMG. The WH is defined as the minimum distance between the lower surface of the HTS bulk and the upper surface of the PMG during the experiment. The central magnetic flux density B_z is an important index to evaluate the magnetic field strength of a magnet guideway. While the unit magnetomotive F_u can be used to compare the PMG and the EMG in terms of energy.

These tests were conducted with a high-precision force-measurement platform. The measurement system has a 3D sliding platform with force sensors, as shown in figure 2. The HTS bulk is a melt textured $\text{YBa}_2\text{Cu}_3\text{O}_7$ (YBCO) pellet with a diameter of 30 mm and a height of 15 mm. Furthermore, In the experimental area of HTS bulk, PMG and EMG have the same size of two-dimensional cross-sectional view. The related parameters are shown in tables 1 and 2.

In experiment 1, under the condition of similar magnetic field structure, three groups of PMG specimens are selected and then through the configuration of current, the central magnetic flux density B_z of the EMG is regulated to be the same as that of the PMG. Specifically, the central magnetic flux density B_z of PMG is measured by gaussmeter and recorded. Adjusting the current of the electromagnet to make the B_z of the EMG is the same as that of the PMG. The main indexes of experiment 1 are shown in table 3.

In experiment 2, under the condition of similar magnetic field structure, three groups of PMG specimens are selected and then adjust the current of the EMG to make the unit magnetomotive F_u of the EMG the same as that of the PMG. There are only two groups here due to iron core deep saturation constraints. Theoretically, the uniform magnetized body can be replaced by an equivalent current-carrying hollow coil. The cross-sectional area and length of the coil are equal to those of the magnet. The magnetomotive of the equivalent coil can be calculated by formula [22]

$$F = NI = ML, \quad (1)$$

where N is the number of turns of the equivalent coil, I is the equivalent current, M is the magnetization intensity of the magnet, and the magnetization intensity M of different magnets can be obtained by simulation. L is the length of the magnet in the direction of magnetizing direction. F is the magnetomotive.

The new evaluation index unit magnetomotive is defined by formula

$$F_u = \frac{F}{A}, \quad (2)$$

where F is the magnetomotive, A is equivalent cross-sectional area of magnetic circuit. The main indexes of experiment 2 are shown in table 4.

2.1. Basic steps of PMG experiments

For the PMG experiments, there were six major steps executed.

Step1: Turn on the power of the high-precision force-measuring platform and make adjustment if necessary;

Step2: Set the distance between the lower surface of the HTS bulk and the upper surface of the PMG specimen 1 as 30 mm;

Step3: Fill liquid nitrogen into the vessel holding the HTS bulk and ensure that the HTS bulk is fully cooled;

Step4: Move the HTS bulk at the speed of 0.5 mm s^{-1} to the WH of 3, 5, and 7 mm respectively, then return to the original WH at the same speed, at last record the levitation force value during the whole tests;

Step5: Measure and record the magnetic flux density at the concerned positions;

Step6: Replace the PMG specimen with specimens 2 and 3 respectively, and repeat the above steps.

2.2. Basic steps of EMG experiments

For the EMG experiments, there were seven major steps executed.

Step1: Turn on the power of the high-precision force-measuring platform and make adjustment if necessary;

Step2: Set the distance between the lower surface of the HTS bulk and the upper surface of the EMG as 30 mm;

Step3: Turn on the DC power supply and set the output current as 0.53 A;

Step4: Fill liquid nitrogen into the vessel holding the HTS bulk and ensure that the HTS bulk is fully cooled;

Step5: Move the HTS bulk at the speed of 0.5 mm s^{-1} to the WH of 3, 5 and 7 mm respectively, then return to the original WH at the same speed, at last record the levitation force value during the whole tests;

Step6: Measure and record the magnetic flux density at the concerned positions;

Step7: Set the exciting current of electromagnet as 1.88, 3.42, 0.94, and 3.41 A respectively, and repeat the above steps.

3. Results and discussion

Experiment 1 is a comparative experiment of the levitation force between PMG and EMG with the same central magnetic flux density B_z . While the experiment 2 is a comparative experiment with the same unit magnetomotive F_u . The experimental results are analyzed and discussed from the two aspects, i.e. the factors affecting the levitation force performance and the comparison between PMG and EMG.

3.1. Results of experiment 1 and experiment 2

Figure 3 shows the results of test 1 and test 4. In these tests, the levitation force was measured with specimen 1 and the exciting currents of 0.53 and 0.94 A at the WHs of 3, 5, and 7 mm, respectively. Figure 4 shows the results of test 2 and test 5. In these tests, the levitation force was measured with specimen 2 and the exciting currents of 1.88 and 3.41 A at the WHs of 3, 5, and 7 mm, respectively. Figure 5 shows the results of test 3. In this test, the levitation force was measured with specimen 3 and the exciting currents of 3.42 A at the WHs of 3, 5, and 7 mm, respectively.

Some important observations should be noticed as follows:

- (1) When the levitation gap is less than a certain height, the levitation force of PMG is much larger than that of EMG with the same central magnetic flux density B_z . When the levitation gap is greater than this height, the results are converse.
- (2) When the unit magnetomotive F_u of EMG and PMG is the same, the levitation force of EMG is always greater than that of PMG.
- (3) With the increase of magnetic flux density, when the PMG and EMG have the same B_z , the levitation gap for

both the samples creating the same levitation force decreases.

- (4) With the increase of magnetic flux density, the difference of maximum levitation force between PMG and EMG with the same B_z is getting smaller, while the difference between PMG and EMG with the same F_u is getting larger.
- (5) The levitation force of EMG changes gently when the HTS bulk approaches the WHs as compared with the results of PMG, whereas it changes steeply when the HTS bulk moves away from the WHs.

3.2. Analysis and discussion

Based on the above observations, three spatial lines are selected to analyze the magnetic field characteristics. The mathematical three-dimensional coordinate equations of spatial lines 1, 2, 3 are shown as notes (3)–(5) respectively

$$\begin{cases} x = 0 \\ y = 0 \\ z = t \end{cases} \quad (0 \leq t \leq 30), \quad (3)$$

$$\begin{cases} x = t \\ y = 0 \\ z = 3 \end{cases} \quad (-20 \leq t \leq 20), \quad (4)$$

$$\begin{cases} x = 0 \\ y = t \\ z = 3 \end{cases} \quad (-20 \leq t \leq 20), \quad (5)$$

where t can be any value in the defined region. Figure 6 shows the actual relative position of the lines 1, 2, 3. The lines 1, 2, 3 can be regarded as z , x and y axis directions respectively, and the intersection point of the lines is the coordinate point (0,0,3). In general, in the longitudinal direction (line 3), the magnet guideway is supposed to have the similar magnetic field distribution. It was verified when measuring the magnetic flux density B_z along line 3, the almost identical results were gotten. Furthermore, practical guideways are long enough to ignore the end effect of the longitudinal direction. As a result, only the magnetic field characteristics in the direction of z -axis (line 1) and x -axis (line 2) were considered.

The basic equation for the levitation force is considered as follows [23]

$$\vec{F}_{lev} = \int_V \vec{J} \times \vec{B}_x dV, \quad (6)$$

where J is the superconducting current density, V is the volume of the induced superconducting current in the HTS bulk, and B_x is x -axis component of magnetic flux density. Intuitively, the levitation force is closely related to B_x . However, it does not mean the magnetic flux density component B_x is the sole dominating factor. According to Faraday's law, J is caused by the change of external magnetic field, which is proportional to the magnetic field

Table 1. Main parameters of PMG.

Brand	Specimen model	Size	Length of magnet in magnetizing direction L	Magnetization intensity M	Coercive force H_c	Remanence B_r	(BH)max
Zhizuan powerful magnet	Specimen 1	100 mm × 20 mm × 2 mm	2 mm	420 kA m ⁻¹	-420 kA m ⁻¹		
	Specimen 2	100 mm × 20 mm × 5 mm	5 mm	610 kA m ⁻¹	-610 kA m ⁻¹	About 12200 Gauss	About 35 MGOe
	Specimen 3	100 mm × 20 mm × 10 mm	10 mm	600 kA m ⁻¹	-600 kA m ⁻¹		

Table 2. Main parameters of EMG.

Parts	Parameters	Values	Unit
Electromagnet iron core	The length of lower arm w_{al}	65	mm
	The height of iron core h	40	mm
Electromagnet coils	Upper coils turns number	1080	
	Lower coils turns number	1592	
	Total resistance	14	ohm
Operational parameters	Rated operating current	4	A
	Rated operation power	224	W

Table 3. The main indexes of experiment 1.

	The central magnetic - flux density B_z	The current of the electromagnet
Test 1	0.0385 T	0.53 A
Test 2	0.1371 T	1.88 A
Test 3	0.2391 T	3.42 A

Table 4. The main indexes of experiment 2.

	The unit magnetomotive F_u	The current of the electromagnet
Test 4	1255.8 kA m ⁻²	0.94 A
Test 5	4555.8 kA m ⁻²	3.41 A
Test 6	8951.2 kA m ⁻²	6.7 A

gradient [24]:

$$J \propto f\left(\frac{\partial B_z}{\partial z}\right) \quad (7)$$

here, the gradient of B_z is simplified as the difference in B_z at the initial and final positions which means that with the same vertical displacement, the greater difference, the stronger superconducting current density. Furthermore, the parameter V increases with the rise of magnetic flux density B_z [24], which can be explained by Bean model. This model assumes that the critical current density J_c is constant, and the correlation analysis based on this model shows that the penetration depth is positively correlated with the B_z , which means the parameter V increases with the rise of B_z . It is clearly that when measuring the levitation force of the HTS bulk at a certain position, the values of magnetic flux density

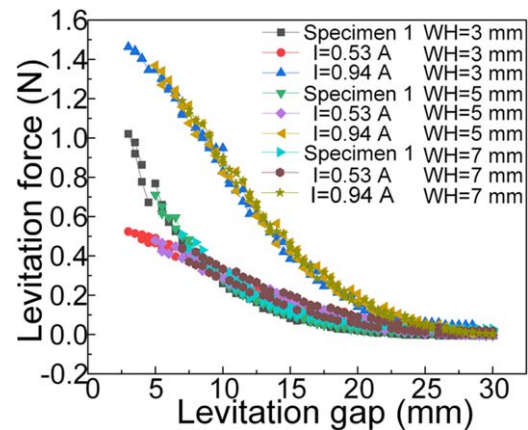


Figure 3. Test results of the levitation force of specimen 1 and EMG with 0.53 and 0.94 A at the WHs of 3, 5, and 7 mm.

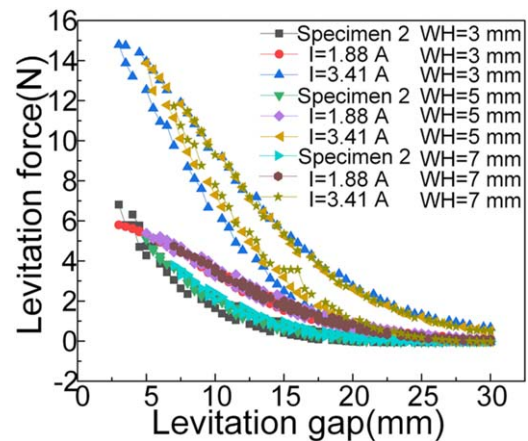


Figure 4. Test results of the levitation force of specimen 2 and EMG with 1.88 and 3.41 A at the WHs of 3, 5, and 7 mm.

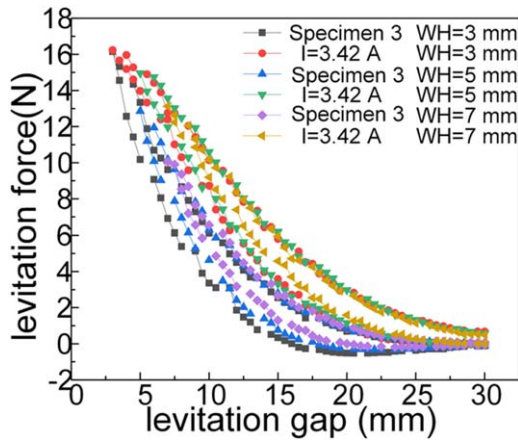


Figure 5. Test results of the levitation force of specimen 3 and EMG with 3.42 A at the WHs of 3, 5, and 7 mm.

components B_z and B_x at that position and the gradient of B_z in the vertical motion direction of the HTS bulk are important. In fact, the HTS bulk with a diameter of 30 mm and a height of 15 mm cannot be seen as an ideal particle point simply. As a result, the difference of B_z is considered in line 1, and the value of B_z and B_x are considered in line 2, which are seen as the main affecting factors.

Based on the above analysis, the comparative study between PMG and EMG with the same central magnetic flux density B_z or unit magnetomotive F_u were analyzed for HTS maglev respectively. Figure 7 are the test results of the difference of magnetic flux density B_z in line 1 of specimen 1, 2, 3 and EMG with current of 0.53, 0.94, 1.88, 3.41, and 3.42 A at the levitation gaps from 0 to 30 mm. The results of magnetic flux density B_z and B_x in line 2 at the lateral displacement from -20 to 20 mm and the levitation gap of 3 mm are shown in figures 8 and 9.

It is easy to see from figures 3, 4, 5 and 7 that compared with the same central magnetic flux density B_z , the variation tendency of levitation force curve is consistent with that of the difference of magnetic flux density B_z curve. Furthermore, with the same central magnetic flux density B_z , when the levitation gap corresponding to the intersection of the force curves decrease, the levitation gap corresponding to the intersection of the difference of B_z curves also decrease. That means when the levitation gap of the same levitation force between PMG and EMG with the same B_z decreases, the gap of the same difference of B_z also decreases. It means the difference of B_z has a great influence on the levitation force performance. It is also noticed the levitation gap corresponding to the same difference of B_z is different from that corresponding to the same levitation force, which means that the levitation force is also affected by other magnetic field characteristics. As a result, the effect of B_z and B_x will be analyzed.

As shown in figures 8 and 9, for the comparative study between PMG and EMG with the same magnetic flux density B_z , the B_z of EMG is always greater than that of PMG, which means a stronger volume V . However, with the same magnetic flux density B_z (experiment 1), the B_x of PMG (as shown

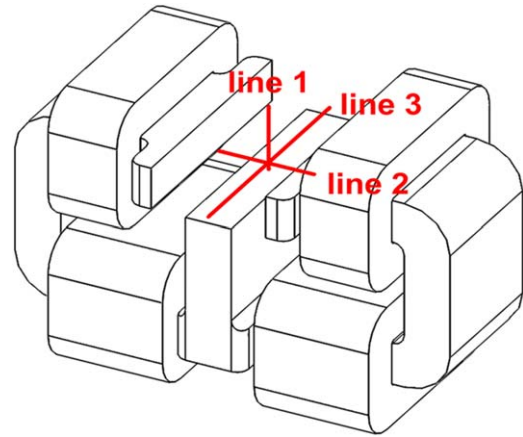


Figure 6. Diagram of relative position of lines 1, 2, 3.

in the black square curve) is greater than that of EMG (as shown in the red circle curve) at the lateral displacement from about -12.5 to 12.5 mm, which can be approximately seen as the edge of the HTS bulk. In this case, with the combined influence of B_z and B_x , PMG can provide a greater levitation force at the levitation gap of 3 mm. Comparing the three groups of tests, with the increase of magnetic field strength, the difference of maximum levitation force between the EMG and the PMG decreases. Furthermore, it is easy to see that when the magnetic field strength increases, the difference of B_z keeps increasing, while the difference of B_x keeps decreasing. Considering the above phenomenon, perhaps it can be analyzed as follows: compared with B_z , B_x has a greater impact on the levitation force performance. As for the comparative study between PMG and EMG with the same unit magnetomotive F_u , the magnetic flux density components B_z and B_x of EMG is always larger than those of PMG. And with the magnetic field strength increasing, the difference of B_z and B_x between PMG and EMG are much larger. As a result, the levitation force of EMG is always stronger than that of PMG and the difference becomes larger.

From the above results and analyses, it is comfortable to conclude that the levitation force performance is closely related to the difference of magnetic flux density component B_z , the value of B_z and B_x . Among them, the difference of B_z , which can reflect the gradient of the B_z , is the most important influence factor, the B_x comes next, and the B_z has the least influence. In summary, perhaps the following possibilities can be considered. Considering the three main factors above, the induced superconducting current density has the largest effect on the levitation force performance, followed by B_x , and the penetration depth of superconducting current in the HTS bulk has the smallest effect with an increased magnetic field strength.

As compared the levitation forces of PMG and EMG with the same magnetic flux density B_z , it is easy to see that the relative magnitude of the levitation force of EMG and PMG varies with the levitation gap. As approaching to the guideway surface, PMG is more likely to provide stronger levitation force performance. As compared the levitation forces of PMG and EMG with the same unit magnetomotive F_u , it is easy to

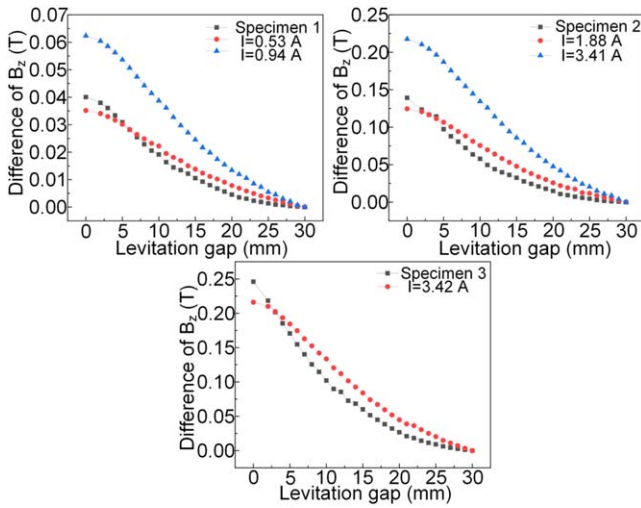


Figure 7. Test results of difference of magnetic flux density B_z of specimen 1, 2, 3 and EMG with current of 0.53, 1.88, 3.42, 0.94, and 3.41 A at the levitation gaps from 0 to 30 mm.

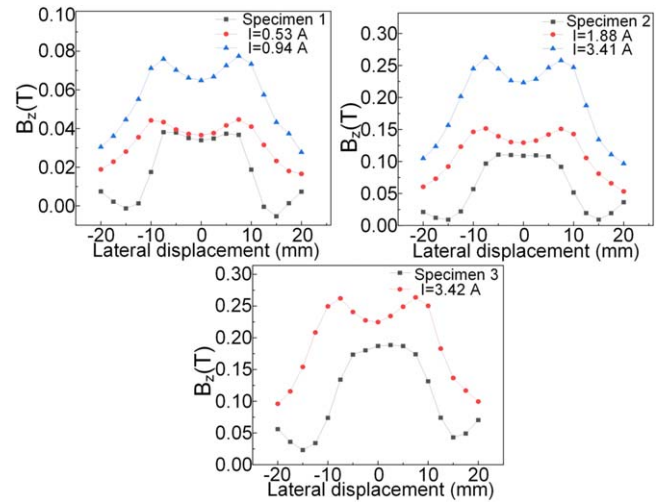


Figure 9. Test results of magnetic flux density B_z of specimen 1, 2, 3 and EMG with current of 0.53, 1.88, 3.42, 0.94, and 3.41 A at the lateral displacement from -20 to 20 mm and the levitation gap of 3 mm.

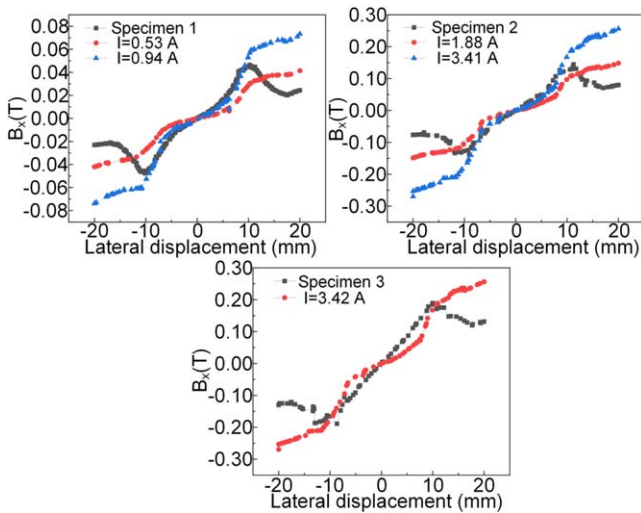


Figure 8. Simulation results of magnetic flux density B_x of specimen 1, 2, 3 and EMG with current of 0.53, 1.88, 3.42, 0.94, and 3.41 A at the lateral displacement from -20 to 20 mm and the levitation gap of 3 mm.

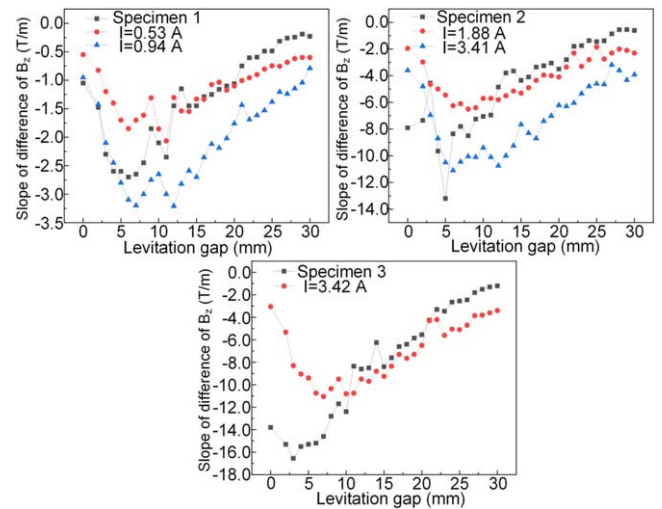


Figure 10. Slopes of the difference of magnetic flux density B_z of line 1 of specimen 1, 2, 3 and EMG at current of 0.53, 1.88, 3.42, 0.94, and 3.41 A at the levitation gaps from 0 to 30 mm.

concluded that the levitation force of EMG is always greater than that of PMG. That means the EMG can provide a larger magnetic field strength when the input energy are same. Specifically, the difference of B_z , B_z and B_x value of EMG is always larger than those of PMG. This can also be seen from the relative magnitude of the exciting current. This means that with the same F_{in} , the EMG can provide stronger magnetic flux density and levitation force.

In fact, the design of EMG model contains iron core, and PMG model is often accompanied with iron plate. That is the characteristic of EMG and PMG. Comparing the levitation force curves of the EMG and the PMG in figures 3–5, an interesting finding is that as close to the guideway surface, the levitation force curve of EMG changes gently, while that of PMG changes rapidly. That means when the vehicle is

running in the WH, the EMG can provide more stable running conditions. Based on the above analyses, the difference of B_z , B_z and B_x are the key factors for the levitation force. The flatness of the curve reflects the change rate of the levitation force. Corresponding, the change rate of levitation force can be seen positively correlated with the change rate of the difference of B_z , which is shown in figure 10. As shown in figure 10, closing to the guideway surface, the absolute value of the slope of the difference of B_z of the black square curve of the PMG model is greater than that of red circle and blue triangle curves of EMG models. While away from the guideway, that of the black square curve is less than that of red circle and blue triangle curves. That means when the HTS bulk is close to the guideway surface, the change rate of the difference of B_z of EMG, which can be reflected by the slope of the curves of the difference of magnetic flux density B_z of

line 1 (shown in figure 10), is always less than that of PMG. While it is away from the guideway, the results converse. Based on the above analyses, it is easy to conclude that EMG can provide stable levitation force which can be seen mainly effected by the slope of difference of B_z .

It is also observed in the experiment that with the same unit magnetomotive F_u , EMG can provide a greater levitation force. However, some demanding requirements are put forward for the magnetic core and coils in EMG design meanwhile.

4. Conclusion

Based on the above experimental results and analyses, some conclusions can be drawn as follows:

- (1) For the levitation force performance, the difference of magnetic flux density B_z along the vertical direction is the key. Flux density along the horizontal direction B_x also affects the magnetic levitation performance. In general, the effect of B_x on levitation force is stronger than that of B_z .
- (2) With the same central magnetic flux density B_z , when the HTS bulk is close to the guideway, PMG can provide a greater levitation force, while levitation force of EMG is more stable. The flatness of levitation force curve is positively correlated with the change rate of the difference of B_z . When the unit magnetomotive F_u of the EMG and PMG is same, EMG can obtain a larger magnetic density and a larger levitation force.
- (3) Some demanding requirements are put forward in EMG design meanwhile.
- (4) Above conclusions will be helpful to the further studies of HTS maglev and provide some guidance for the subsequent EMG design.

ORCID iDs

Yuyan Wen  <https://orcid.org/0000-0002-3979-9716>

Ying Xin  <https://orcid.org/0000-0001-7835-3832>

Wei Hong  <https://orcid.org/0000-0002-9656-7727>

References

- [1] Wang J S *et al* 2005 The present status of the high temperature superconducting maglev vehicle in China *Supercond. Sci. Technol.* **18** S215–8
- [2] Huang C G *et al* 2019 Dynamic simulations of actual superconducting maglev systems considering thermal and rotational effects *Supercond. Sci. Technol.* **32** 045002
- [3] Wang X *et al* 2012 Numerical analyses of the electromagnetic force acting on high-temperature superconducting power cables due to fault current *Supercond. Sci. Technol.* **25** 054018
- [4] Heydari H *et al* 2008 Superconducting technology for overcurrent limiting in a 25 kA current injection system *Supercond. Sci. Technol.* **21** 095016
- [5] Strasik M *et al* 2010 An overview of Boeing flywheel energy storage systems with high-temperature superconducting bearings *Supercond. Sci. Technol.* **23** 034021
- [6] Zhang W F *et al* 2019 Magnetic levitation and guidance performance of Y–Ba–Cu–O and Gd–Ba–Cu–O bulk superconductors under low ambient pressure *Supercond. Sci. Technol.* **52** 365001
- [7] Rudnev I *et al* 2019 The influence of cyclical lateral displacements on levitation and guidance force for the system of coated conductor stacks and permanent magnets *Supercond. Sci. Technol.* **6** 036001
- [8] Li H *et al* 2019 Lateral motion stability of high-temperature superconducting maglev systems derived from a nonlinear guidance force hysteretic model *Supercond. Sci. Technol.* **31** 075010
- [9] Jiang F J *et al* 2019 Optimization analysis of minimum flat curve radius of high speed maglev line with design speed of 500 km h⁻¹ *Supercond. Sci. Technol.* **637** 012008
- [10] Schultz L *et al* 2005 Superconductively levitated transport system—the SupraTrans project *IEEE Trans. Appl. Supercond.* **15** 2301–5
- [11] Huang C G *et al* 2019 Numerical analysis of the influence of superconductor and magnet material parameters on the dynamic stability of maglev systems *Supercond. Sci. Technol.* **649** 012026
- [12] Zhao L *et al* 2019 Attenuation of levitation performance for side-suspending HTS maglev system under vibration *IEEE Trans. Appl. Supercond.* **29** 3603105
- [13] Ma G, Wang J and Wang S 2010 Numerical investigation of the lateral movement influence on the levitation force of the bulk HTS based on a 3D model *IEEE Trans. Appl. Supercond.* **20** 924–8
- [14] Zheng J *et al* 2007 Stability of the maglev vehicle model using bulk high T_c superconductors at low speed *IEEE Trans. Appl. Supercond.* **17** 2103–6
- [15] Sun R *et al* 2016 Study on the magnetic field inhomogeneity of a Halbach permanent-magnet guideway due to different defects *IEEE Trans. Appl. Supercond.* **26** 3600107
- [16] Ishihara A *et al* 2017 Superior homogeneity of trapped magnetic field in superconducting MgB₂ bulk magnets *Supercond. Sci. Technol.* **30** 035006
- [17] Wang H *et al* 2006 Analysis for ring arranged axial field Halbach permanent magnets *IEEE Trans. Appl. Supercond.* **16** 1562–5
- [18] Deng Z *et al* 2008 High-efficiency and low-cost permanent magnet guideway consideration for high- T_c superconducting maglev vehicle practical application *Supercond. Sci. Technol.* **21** 115018
- [19] Ozturk K *et al* 2015 The effect of magnetic field distribution and pole array on the vertical levitation force properties of HTS maglev systems *IEEE Trans. Appl. Supercond.* **25** 3601607
- [20] Baskys A, Patel A and Glowacki B A 2018 Measurements of crossed-field demagnetisation rate of trapped field magnets at high frequencies and below 77 K *Supercond. Sci. Technol.* **31** 065011
- [21] Liu L *et al* 2010 Levitation force transition of high- T_c superconducting bulks in varying external magnetic field *IEEE Trans. Appl. Supercond.* **20** 920–3
- [22] Jiao L C and Cheng Z P 2014 *Operating Characteristics and Control of Permanent Magnet Liner Synchronous Motor* (Beijing, China: Science Press) pp 24–6
- [23] Chen W *et al* 2018 Levitation force computation of HTS/PM system based on H-Formulation *IEEE Trans. Magn.* **54** 7402805
- [24] Liu W *et al* 2008 Levitation performance of YBCO bulk in different applied magnetic fields *Physica C* **468** 974–7